Track Reconstruction Algorithm at Level-1 Trigger for High Luminosity upgrade

Month-4 Master's Thesis Report

Nivedaa Dhandapani

Supervisor: Dr. Ritesh Singh

Abstract

One of the major challenges with the advent of the High Luminosity(HL) upgrade at the LHC is analysing and storing input data which is expected to increase ten-fold. There is also a significant increase in the number of pile-ups which makes vertex reconstruction more inaccurate with existing algorithms. In this project, we develop a track reconstruction algorithm using the information from the tracks made available at the Level-1(L1) trigger by the HL upgrade. On evaluating various link and track parameters computed using coordinate information from track layers, clustering patterns are identified in both real and reconstructed momentum spaces. These patterns are used to further form links and "tracklets" from points which become the track candidates during reconstruction.

Contents

1 Introduction

The Large Hadron Collider (LHC) today has luminosity of $10^{34} cm^{-2} s^{-1}$ and an integrated luminosity of $300 fb^{-1}$. High Luminosity(HL) upgrade of the LHC is scheduled for completion and operation in 2029 and the Compact Muon Solenoid(CMS) will observe an integrated luminosity of $3ab^{-1}$ which is 10 times the current value. To put things in perspective, the trigger now has to sort 10 times more data for each bunch crossing which occurs every 25 ns. The data storage system at the L1 trigger level can hold the data for upto 6 μs to perform online analysis after which that data is discarded to make room for new events and collisions. The HL upgrade will now introduce availability of tracker data at l1 trigger which previously only consisted of calorimeter and muon spectrometer data.In this project, we try to develop an ultrafast algorithm which can use tracker data to sift through this massive influx of data.

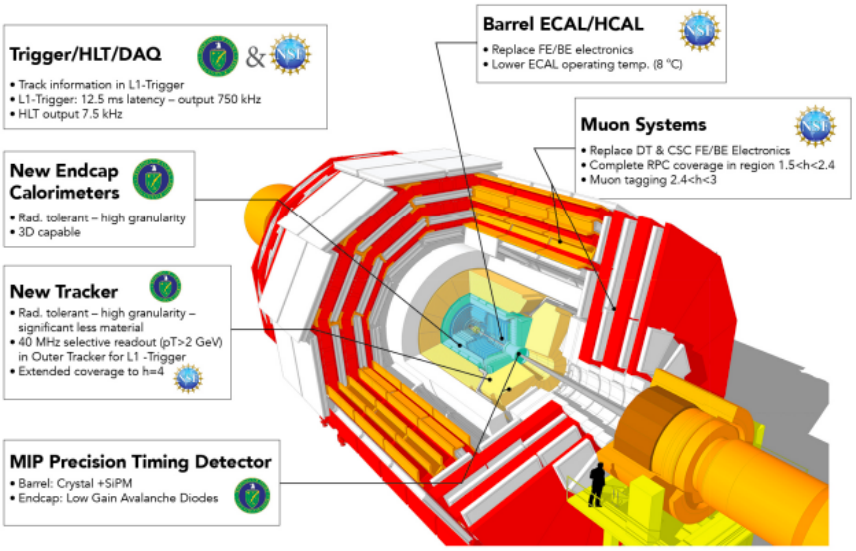

Figure 1: High-Luminosity upgrade of CMS

1.1 Trajectory for a Charged Particle in the Detector

The CMS detector maintains a strong uniform magnetic field within the beam pipe passing through the centre of the structure. When the proton bunches cross in LHC at the location of the CMS detector, the charged particles produced as a result of this high energy collision are deflected by the uniform magnetic field along the direction of beam line as (denoted by the diagram above). In order to understand the trajectory, we must study the case of a charged particle in constant uniform magnetic field. Let the particle have initial energy-momentum contravariant tensor p^α given by

$$p^\alpha = \left\{ \frac{\mathcal{E}}{c}, \mathbf{p} \right\} = \gamma \left\{ mc, \mathbf{p} \right\} = m \frac{dx^\alpha}{d\tau} \equiv m u^\alpha \tag{1}$$

where u^α is the contravariant form on the four-velocity of the particle given by $u^\alpha = \frac{dx^\alpha}{d\tau}$ and τ is the proper time given by $d\tau = \frac{dt}{\gamma}$.

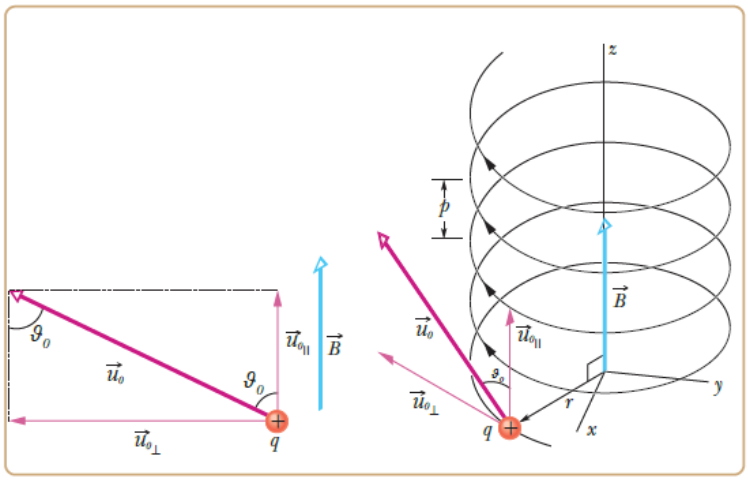

Figure 2: Trajectory of charged particle in constant and uniform magnetic field

The particle's dynamics in four-form is given by the four-vector equality (which is evidently form-invariant with respect to the Lorentz transformation):

$$\frac{dp^{\alpha}}{d\tau} = qF^{\alpha\beta}u_{\beta} \tag{2}$$

where q is the charge of the relativistic particle of interest and $F^{\alpha\beta}$ is the Maxwell's tensor.

The equation (2) for the case of uniform and constant magnetic field($\mathbf{E} = 0$) reads for each component of the 3-momentum vector as:

$$\frac{dp^{i}}{d\tau} = qF^{i\beta}u_{\beta} = q\gamma\left[\mathbf{E} + \mathbf{u}\times\mathbf{B}\right]_{a} = q\gamma\left[\mathbf{u}\times\mathbf{B}\right]_{a} \quad \forall(i,a) = (1,x),(2,y),(3,z) \tag{3}$$

Recalling $p^0 = \frac{\mathcal{E}}{c}$, $d\tau = \frac{dt}{\gamma}$ and substituting in $\frac{dp^0}{d\tau} = qF^{0\beta}u_{\beta}$, we get the particle's energy evolution:

$$\frac{d\mathcal{E}}{c} = q\mathbf{E}\cdot\mathbf{u} = 0 \tag{4}$$

Equation (4) gives $\mathcal{E}$ is constant from which we get $|\mathbf{u}| = u$ is constant, $\beta\ \frac{u}{c}$ is constant, $\gamma = (\sqrt{1-\beta^2})^{-1}$ is constant and finally $M = \gamma m$ is constant. From this we can rewrite equation (3) as,

$$\frac{dp}{dt} = \mathbf{u}\times\boldsymbol{\omega_c} \tag{5}$$

where $\boldsymbol{\omega_c}$ is the vector directed along the magnetic field $\mathbf{B}$, whose magnitude is equal to the following cyclotron frequency:

$$\omega_c \equiv \frac{qB}{M} = \frac{qB}{\gamma m} = \frac{qc^2B}{\mathcal{E}} \tag{6}$$

The cyclotron motion's radius can be calculated as $R = \frac{u_{\perp}}{\omega_c}$ We can represent this in terms of momentum as:

$$R = \frac{\gamma m u_{\perp}}{qB} = \frac{p_{\perp}}{qB} \tag{7}$$

The particle motion is unencumbered in the direction parallel to magnetic field and it's displacement along the z-direction can be represented as

$$\Delta z = u_{\parallel} t = \frac{p_{\parallel}}{\gamma m} t \tag{8}$$

From the above trajectory equations we can conclude that the relativistic charged particle follows a helical path in constant uniform magnetic field inside the detector. This can represented in the parametric form in time as:

$$x = x_c + Rcos\omega_c t, y = y_c + Rsin\omega_c t, z = z_0 + u_z t \tag{9}$$

(or)

$$x = x_0 + R_x sin\omega_c t + R_y(1 - cos\omega_c t), y = y_0 - R_x(1 - cos\omega_c t) + R_y sin\omega_c t, z = z_0 + u_z t \tag{10}$$

Here (u_x, u_y, u_z) is the three-velocity of the particle and we take $\omega_c t = \phi$, $R_x = u_x/\omega_c$ and $R_y = u_y/\omega_c$ Equation (9) represents the trajectory taking (x_c, y_c) as the centre of the helix and z_0 as the inital point of the helix in z whereas equation (10) represents the trajectory in terms of the initial point on the helix given by (x_0, y_0, z_0). The results are very similar to what is expected from a non-relativistic case.

1.2 Defining input co-ordinates

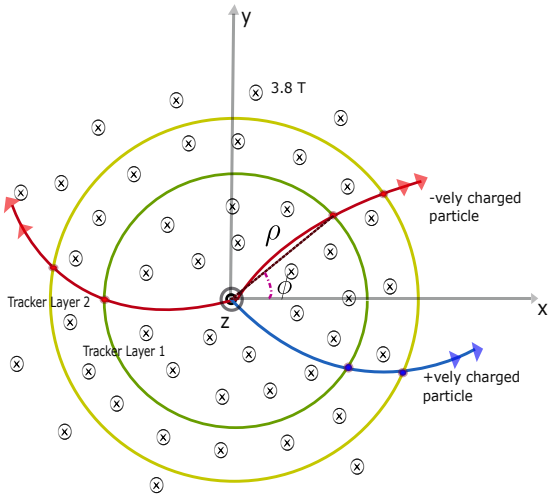

Figure 3: Cross section of the detector showing how ρ and ϕ are measured

The best co-ordinate system to represent a helix is a cylindrical co-ordinate system with its origin at the centre of the beam pipe along the middle of the detector. We define the cylindrical co-ordinates (ρ, ϕ, z) with respect to Cartesian co-ordinates (x, y, z) as:

$$\rho = \sqrt{x^2 + y^2}$$

$$\phi = tan^{-1}(y/x)$$

$$z = z$$

When a charged particle passes through one of the detector layers, we record it's Cartesian co-ordinate as (x_i^n, y_i^n, z_i^n) with respect to origin as defined in the above paragraph. Here n represents the particle number passing through the 'i^{th}' later of the tracker. With this information we calculate ρ_i^n and ϕ_i^n as:

$$\rho_i^n = \sqrt{(x_i^n)^2 + (y_i^n)^2}$$

$$\phi_i^n = tan^{-1}(y_i^n/x_i^n)$$

Particle physicists also use a quantity called pseudorapiditiy η, a spatial co-ordinate which describes the angle of a particle relative to the beam axis. It is defined as:

$$\eta \equiv -ln\left[tan\left(\frac{\theta}{2}\right)\right]$$

where θ is the angle between the particle three-momentum $\mathbf{p}$ and the positive direction of the beam axis (see figure 4.

We also define a transverse plane as plane perpendicular to the beam line. Parameters measured in this direction are identified with their subscript (X_T)) We represent the three momentum of the particle along the transverse plane as transverse momentum denoted by p_T and three momentum along the beam line as z-momentum denoted by p_z. In the next section, we will motivate the derivation of geometric variables from the above defined co-ordinate systems which will subsequently used for clustering.

2 Deriving Clustering Variables

2.1 Definitions

Before we dive into understanding the idea behind finalising and deriving clustering geometric variables, let us define a nomenclature for this report:

- Input points/points refer to the co-ordinates at which a moving charged particle interacted with a tracker layer.
- Links are made by connecting two points. In the subsequent sections we will only be creating links between two points on the consecutive layers of the tracker.
- A tracklet is made by connecting two links which share a common point. It consists of three points and two links in total.

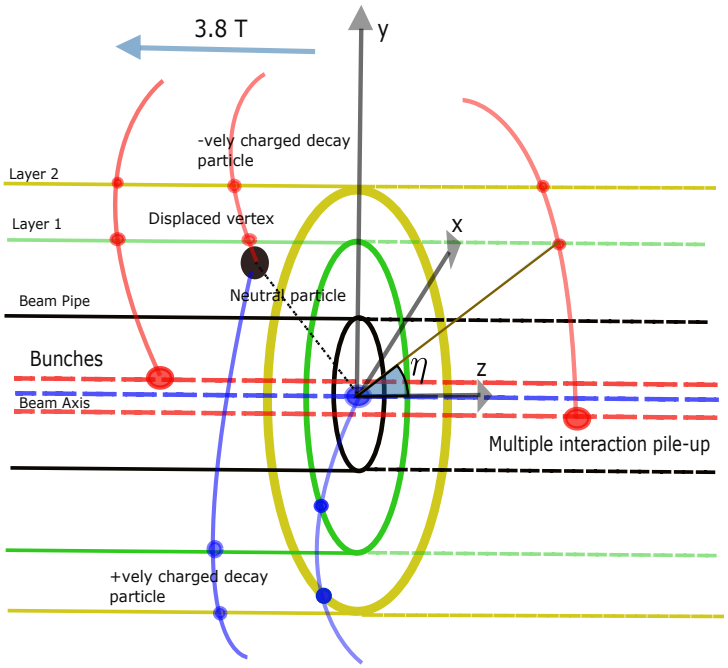

Figure 4: Side view of the detector showing two innermost tracker layers, displaced vertices and how θ is measured. Red is negatively charged particle and blue is positively charged particle.

2.2 Motivation

In order to uniquely construct a helix one must require 6 parameters (verified from equations (9) and (10)) which are :

- $(x_0, y_0, z_0) \implies$ 3 parameters which represent starting point on the helix

  (or)

  $(x_c, y_c, z_0) \implies$ 2 parameters (x_c, y_c) for the centre of the helix + 1 parameter z_0 to represent starting point on the helix only in z-direction.

- $R \implies$ 1 parameter for the radius of the helix.

- $\phi \implies$ 1 parameter to represent azimuthal angle.

- $u_z \implies$ 1 parameter to represent change in z-direction with respect to time.

We can represent these parameters $(x_0, y_0, z_0, u_z, R, \phi)$ in terms of the three-momenta p_T and p_z using the relations 7,8 to give $(x_0, y_0, z_0, p_z, p_\perp, \phi)$ as the new set of parameters defining a helix uniquely.

Since we will only consider high energy particles which experience minimal energy loss when interacting with the different tracker layers, we can assume the p_T and p_z of the tracks to be high and nearly equal throughout the journey of the particle through the detector. This means for a unique helical track reconstructed, its derived p_T and p_z must remain almost

constant. Therefore, the derived variables which are proportional to p_T and p_z must cluster in reconstructed momentum space with each cluster closely resembling a real track.

We have therefore substantiated our motivation to look for the geometric variables which are proportional to p_z and p_T

2.3 Analytical Expressions

2.3.1 Geometric Variables

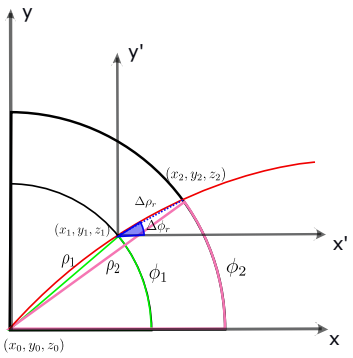

Figure 5: Illustration on difference between lab and relative co-ordinate difference of ϕ and ρ

On the search for geometric variables which can be defined for a link consisting of two input points, we sampled various ratios of differences of co-ordinates such as $\frac{\Delta\phi}{\Delta\eta} := \frac{\phi_i - \phi_j}{\eta_i - \eta_j}$, $\frac{\Delta\eta}{\Delta z} := \frac{\eta_i - \eta_j}{z_i - z_j}$, $\frac{\Delta\eta}{\Delta x} := \frac{\eta_i - \eta_j}{x_i - x_j}$ $\frac{\Delta\rho}{\Delta\eta} := \frac{\rho_i - \rho_j}{\eta_i - \eta_j}$ etc. The i,j represent the layer number of the co-ordinate.

After analysing the clustering patters, the final set of geometric variables picked were:

$$\frac{\Delta\phi}{\Delta z} := \frac{\phi_i - \phi_j}{z_i - z_j}, \frac{\Delta\rho}{\Delta z} := \frac{\rho_i - \rho_j}{z_i - z_j}, \frac{\Delta\phi}{\Delta\rho} := \frac{\phi_i - \phi_j}{\rho_i - \rho_j} \tag{11}$$

Using equations (6), (8), $\phi_i = \omega_c t_i$ and $\rho_i = \frac{p_T}{\gamma m} t_i$, we get the analytical expressions for the final three variables as:

$$\frac{\phi_i - \phi_j}{z_i - z_j} \approx \frac{qB}{\gamma m u_z} \left(\frac{t_i - t_f}{t_i - t_f} \right) = \frac{qB}{p_z} \tag{12}$$

$$\frac{\rho_i - \rho_j}{z_i - z_j} \approx \frac{u_T}{u_z} \left(\frac{t_i - t_f}{t_i - t_f} \right) = \frac{p_T}{p_z} \tag{13}$$

$$\frac{\phi_i - \phi_j}{\rho_i - \rho_j} \approx \frac{qB}{\gamma m u_T} \left(\frac{t_i - t_f}{t_i - t_f} \right) = \frac{qB}{p_T} \tag{14}$$

We can see the direct or inverse proportionality to p_z and p_T for the chosen variables. One thing to keep in mind here is that tee equations are an approximation which hold only for high p_T, low ω_c tracks. The general case equations are a lot more complex and will be dealt with in the next part of the project.

A key detail is that all these co-ordinates are in "lab" frame i.e, origin is at the centre of the beam line of the detector. In an ideal scenario, all collisions take place at a singular point and we can shift our co-ordinate system to have its origin at this single interaction point keeping all the analysis unchanged. Unfortunately, we neither have ideal detectors nor beams and therefore observe the interaction vertex displaced for most collisions (shown in figure 4). This tampers with clustering results.

In order to solve the problem of displaced vertices, we introduce of the idea of relative co-ordinate difference where the co-ordinates such as ρ, ϕ of one point on a link are measured from the other point on the same link (see figure 5). *(To fully appreciate this subtlety, see figure 7).* The analytical expression of $\Delta\phi_r$ and $\Delta\rho_r$ in terms of Cartesian co-ordinates are:

$$\Delta\phi_r = tan^{-1}\left(\frac{y_i - y_j}{x_i - x_j}\right) \tag{15}$$

$$\Delta\rho_r = sqrt(x_i - x_j)^2 + (y_i - y_j)^2 \tag{16}$$

Incidentally, relative co-ordinate difference of z Δz_r is the same as Δz since in the relative frame the shift in z cancel each other returning the "lab" frame value. Relative co-ordinate difference of ρ, $\Delta\rho_r$ and $\Delta\rho$ show barely any change from each other. We will stick to lab frame for differences of all co-ordinates of the input points except ϕ.

2.3.2 Vertex Reconstruction

There can exist two tracks which exhibit every similar behaviour in $\rho-\phi$ plane but be separated in z. This becomes difficult since the three clustering variables that were finalised in the previous part lose any information on z vertex since we use Δz. To solve this issue, we need to reconstruct the co-ordinate interaction vertex along the z-direction. $\frac{\Delta\rho_l}{\Delta z}$ is constant for a given track, we can hence represent a line of the form:

$$\rho_f - \rho_i = \frac{\Delta\rho_l}{\Delta z}(z_f - z_i) \tag{17}$$

For $\rho_i = 0$, z_i is the z co-ordinate of the vertex, let us say z_0.

Therefore we get:

$$z_0 = z_f - \left(\frac{\Delta\rho_l}{\Delta z}\right)^{-1}\rho_f \tag{18}$$

Now we can distinguish two vertices along the z-axis!

3 Plots

The data for this analysis was generated using bijection method to solve for the points of intersection randomly generated helical particle trajectory with concentric tracker layers. We took 10 layers each with increasing radius of 0.1m centered at the origin of the co-ordinate system. A particle can start randomly anywhere in the range of $x \in (-5\text{cm}, 5\text{cm})$, $y \in (-1\text{cm}, 1\text{cm})$ and $z \in (-10\text{cm}, 10\text{cm})$ (this choice is arbitrary and just made to demonstrate the robustness of the clustering). After simulating 500 track, we chose the first 20 tracks to visualise as 2D plots.

Figure 6 shows the plots of the three finalised geometric variables and track paramteres in various combinations. From a quick glance we can conclude that the plot $\frac{\Delta\rho_l}{\Delta z_l}$ vs $\frac{\Delta\phi_r}{\Delta z_l}$ has the tightest clustering out of all of them.

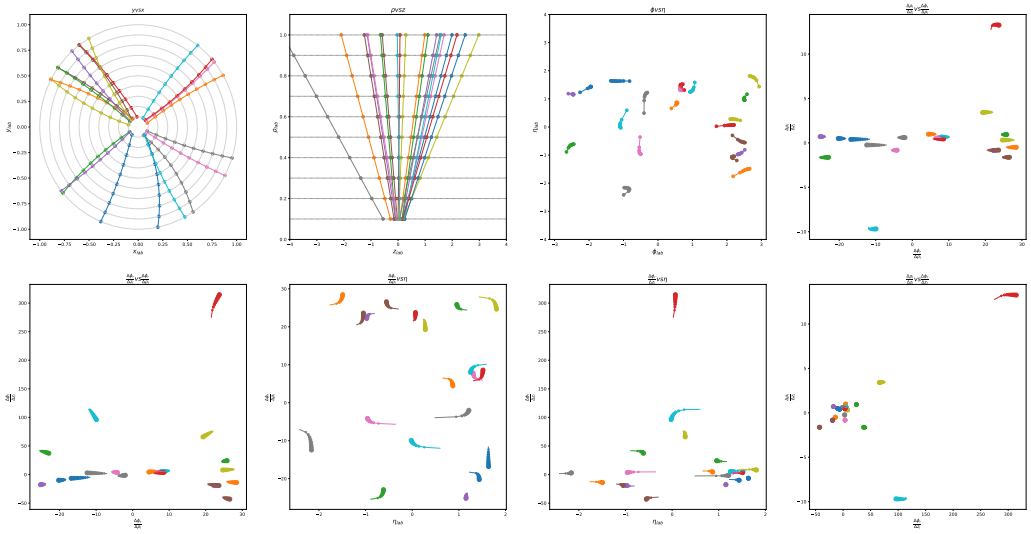

Figure 6: TOP from left to right:y vs x, ρ vs z, ϕ vs η, $\frac{\Delta\rho_l}{\Delta z_l}$ vs $\frac{\Delta\phi_r}{\Delta\rho_l}$.
BOTTOM from left to right: $\frac{\Delta\phi_r}{\Delta z_l}$ vs $\frac{\Delta\phi_r}{\Delta\rho_l}$, $\frac{\Delta\phi_r}{\Delta\rho_l}$ vs η, $\frac{\Delta\phi_r}{\Delta z_l}$ vs η, $\frac{\Delta\rho_l}{\Delta z_l}$ vs $\frac{\Delta\phi_r}{\Delta z_l}$

Let us compare the geometric variable with relative co-ordinate difference of ϕ, $\Delta\phi_r$ against $\Delta\phi_l$ where subscript l denotes "lab" frame. In the figure 7, we immediately notice that the clustering in $\frac{\Delta\rho_l}{\Delta z_l} vs \frac{\Delta\phi_r}{\Delta z_l}$ plot (to the left) is way cleaner than $\frac{\Delta\rho_l}{\Delta z_l} vs \frac{\Delta\phi_l}{\Delta z_l}$ plot (to the right). Moving forward we will restrict ourselves to analysing variables with $\Delta\phi_r$.

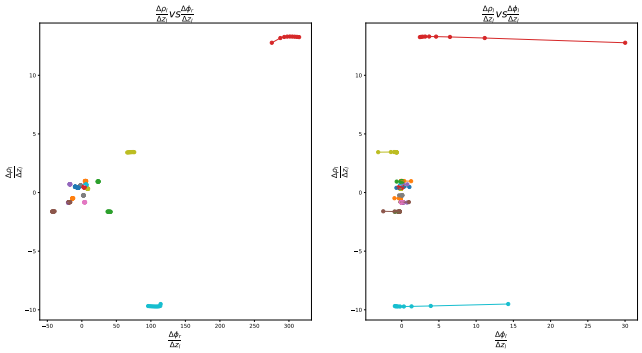

Figure 7: $\frac{\Delta\rho_l}{\Delta z_l}$ vs $\frac{\Delta\phi_r}{\Delta z_l}$ (left), $\frac{\Delta\rho_l}{\Delta z_l}$ vs $\frac{\Delta\phi_l}{\Delta z_l}$ (right).

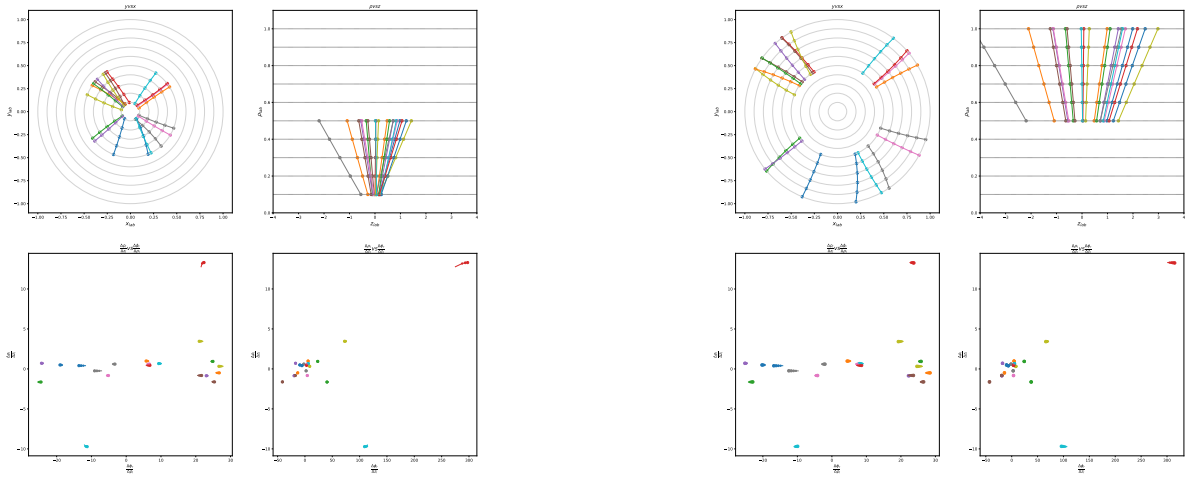

(a) Inner track links

(b) Outer track links

Figure 8: TOP left to right: y vs x, ρ vs z.
BOTTOM left to right: $\frac{\Delta\rho_l}{\Delta z_l}$ vs $\frac{\Delta\phi_r}{\Delta\rho_l}$, $\frac{\Delta\rho_l}{\Delta z_l}$ vs $\frac{\Delta\phi_r}{\Delta z_l}$

In order to figure out a clustering strategy we plotted the behaviour of two best geometric variables for different parts of the track - the inner four links and outer five links. In figure 8 we have represented two plots 8a and 8b for inner and outer layers respectively. Upon inspection, we see that the clustering is stronger and more robust for links in the outer layers of the tracker than for those in the inner layers (see the top right corner track shown in red to show anomalous behaviour in inner tracks but more compact in outer tracks). This inference gives the idea that linking up tracklets from outside in would be a more effective approach towards track reconstruction.

4 Next Step

- We will be creating a class that will take Cartesian co-ordinates and give point object which consists of representation in cylindrical co-ordinates and calculates which layer of the tracker it is present. Then this point object will be input into a class which forms links based on whether given two points are in consecutive layers of the detector. This will output a link object consisting of geometric variables calculated for that particular link. Then this object will be passed into a tracklet class which will make three point trackets joining any two links with a common point.

- We verify the tracklets formed against on tightness of clustering in 3D cluster space and find more links which could be potenital candidates for extending the track to completion.

- We will be testing this algorithm out on simulated data to tailor it to fit the geometry of the detector.

- We will be implementing the algorithm on an Field Programmable Gate Array and work to imorove its efficency.

References

[1] Lieret, K., et al. (2023). *High Pileup Particle Tracking with Object Condensation* https://arxiv.org/pdf/2312.03823.pdf

[2] Lieret, K., et al. (2023). *An Object Condensation Pipeline for Charged Particle Tracking at the High Luminosity LHC* https://arxiv.org/pdf/2309.16754.pdf